

# POINT CONFIGURATIONS AND BLOW-UPS OF COXETER COMPLEXES

SUZANNE M. ARMSTRONG, MICHAEL CARR, SATYAN L. DEVADOSS, ERIC ENGLER, ANANDA LEININGER, AND MICHAEL MANAPAT

ABSTRACT. The minimal blow-ups of simplicial Coxeter complexes are natural generalizations of the real moduli space of Riemann spheres. They inherit a tiling by the graph-associahedra convex polytopes. We obtain configuration space models for these manifolds (of spherical and Euclidean Coxeter type) using particles on lines and circles. A (Fulton-MacPherson) compactification of these spaces is described and an operad-like structure is shown to appear. An enumeration of the building sets of these complexes is also given with an algorithm to compute the Euler characteristics.

## 1. MOTIVATION FROM PHYSICS

A configuration space of  $n$  ordered, distinct particles on a variety  $V$  is defined as

$$C_n(V) = V^n - \Delta, \quad \text{where } \Delta = \{(x_1, \dots, x_n) \in V^n \mid \exists i, j, x_i = x_j\}.$$

Recent work in physics has led to an increased interest in the configuration space of  $n$  labeled points on the projective line. The focus is on a quotient of this space by  $\mathbb{P}\mathrm{GL}_2(\mathbb{C})$ , the affine automorphisms on  $\mathbb{C}\mathbb{P}^1$ . The resulting variety is the moduli space of Riemann spheres with  $n$  punctures

$$\mathcal{M}_0^n(\mathbb{C}) = C_n(\mathbb{C}\mathbb{P}^1)/\mathbb{P}\mathrm{GL}_2(\mathbb{C}).$$

There is a Deligne-Knudsen-Mumford compactification  $\overline{\mathcal{M}}_0^n$  of this space, a smooth variety of complex dimension  $n - 3$ , coming from Geometric Invariant Theory and appearing in the theory of Gromov-Witten invariants, symplectic geometry, and quantum cohomology. Our work is motivated by the *real* points  $\overline{\mathcal{M}}_0^n(\mathbb{R})$  of this space, the set of points fixed under complex conjugation.

It was Kapranov [12] who first noticed a relationship between  $\overline{\mathcal{M}}_0^n(\mathbb{R})$  and the braid arrangement of hyperplanes, associated to the Coxeter group of type  $A_n$ : Blow-ups of certain cells of the  $A_n$  Coxeter complex yields a space homeomorphic to  $\overline{\mathcal{M}}_0^n(\mathbb{R})$ . This creates a natural tiling of  $\overline{\mathcal{M}}_0^n(\mathbb{R})$  by associahedra, the combinatorics of which is discussed in [10]. Davis et. al have generalized this to all Coxeter groups [5], along with studying the fundamental groups of these spaces [6]. Carr and Devadoss [4] looked at the simplicial

---

1991 *Mathematics Subject Classification*. Primary 52C35, Secondary 14P25, 52B11.

All authors were partially supported by NSF grant DMS-9820570. Carr and Devadoss were also supported by NSF CARGO grant DMS-0310354.

Coxeter groups with the inherent tiling of these spaces by the convex polytopes *graph-associahedra*. Below, a configuration space analog of these blown-up Coxeter complexes is given along with a corresponding (Fulton-MacPherson) compactification. An operad-like structure appears from this compactification.

2. SPHERICAL AND EUCLIDEAN COMPLEXES

2.1. We begin with some standard facts and definitions about Coxeter systems. Most of the background used here can be found in Bourbaki [2] and Brown [3].

**Definition 2.1.** Given a finite set  $S$ , a *Coxeter group*  $W$  is given by the presentation

$$W = \langle s_i \in S \mid s_i^2 = 1, (s_i s_j)^{m_{ij}} = 1 \rangle,$$

where  $m_{ij} = m_{ji}$  and  $2 \leq m_{ij} < \infty$ . The pair  $(W, S)$  is called a *Coxeter system*.

A Coxeter group is *simplicial* if it is irreducible and locally finite; the classification of simplicial Coxeter groups is well-known [2]. We restrict our attention to infinite families of simplicial Coxeter groups which generalize to arbitrary number of generators. This will mimic configuration spaces of an arbitrary number of particles since our motivation comes from  $\overline{\mathcal{M}}_0^n(\mathbb{R})$ . There are only seven such types of Coxeter groups: three spherical ones and four Euclidean ones.

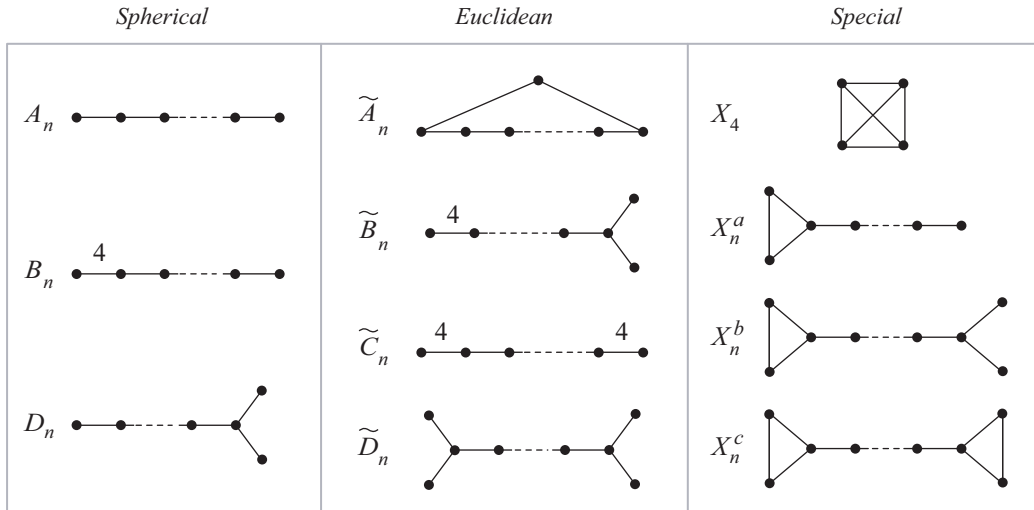


TABLE 1. Coxeter graphs of spherical and Euclidean groups, along with special cases.

Associated to any Coxeter system  $(W, S)$  is its *Coxeter graph*  $\Gamma_W$ : Each node represents an element of  $S$ , and two nodes  $s_i, s_j$  determine an edge if and only if  $m_{ij} \geq 3$ . We label the edge with its order for  $m_{ij} > 3$ . The first two columns of Table 1 show the Coxeter graphs

associated to the Coxeter groups of interest. The number of nodes of a graph is given by the subscript  $n$  for the spherical groups, whereas the number of nodes is  $n + 1$  for the Euclidean case.

2.2. Every simplicial Coxeter group has a realization as a group generated by reflections acting faithfully on a variety. The geometry of the variety is either spherical, Euclidean, or hyperbolic, depending on the group. Every conjugate of a generator  $s_i$  acts on the variety as a reflection in some hyperplane, dividing the variety into simplicial chambers. This variety, along with its cellulation is the *Coxeter complex* corresponding to  $W$ , denoted  $\mathcal{C}W$ .

Every spherical Coxeter group has an associated finite reflection group realized by reflections across linear hyperplanes on a sphere. Our focus is on the infinite families of such spherical Coxeter groups which are the three types  $A_n$ ,  $B_n$  (also known as  $C_n$ ), and  $D_n$ . The hyperplanes associated to each group, given in Table 2, lies on the  $(n - 1)$  sphere. The  $W$ -action on the chambers of  $\mathcal{C}W$  is transitive, and thus we may associate an element of  $W$  to each chamber; generally, the identity is associated to the fundamental chamber. Thus the number of chambers of  $\mathcal{C}W$  comes from the order of the group.

$W$	Hyperplanes	# Chambers
$A_n$	$x_i = x_j$	$(n + 1)!$
$B_n$	$x_i = \pm x_j, x_i = 0$	$2^{n-2} (n + 1)!$
$D_n$	$x_i = \pm x_j$	$2^{n-3} (n + 1)!$

TABLE 2. The spherical complexes.

Figure 1(a) is  $\mathcal{C}A_3$ , the 2-sphere with hyperplane markings, and Figure 1(b) is the 2-sphere  $\mathcal{C}B_3$ . Note that both of them are tiled by 2-simplices.



FIGURE 1. Coxeter complexes (a)  $\mathcal{C}A_3$ , (b)  $\mathcal{P}\mathcal{C}A_3$  and (c)  $\mathcal{C}B_3$ .

2.3. We move from spherical geometry coming from linear hyperplanes to Euclidean geometry arising from affine hyperplanes. Just as with the spherical case, each Euclidean Coxeter group has an associated Euclidean reflection group realized as reflections across affine hyperplanes in Euclidean space. Again, we focus on the infinite families of such Euclidean

Coxeter groups which are  $\tilde{A}_n, \tilde{B}_n, \tilde{C}_n$ , and  $\tilde{D}_n$ . The hyperplanes associated to each group, given in Table 3, lies in  $\mathbb{R}^n$ .

$W$	Hyperplanes ( $k \in 2\mathbb{Z}$ )	# Chambers
$\tilde{A}_n$	$x_i = x_j + k$	$n!$
$\tilde{B}_n$	$x_i = \pm x_j + k, x_i = 1 + k$	$2^n n!$
$\tilde{C}_n$	$x_i = \pm x_j + k, x_i = 1 + k, x_i = 0 + k$	$2^{n+1} n!$
$\tilde{D}_n$	$x_i = \pm x_j + k$	$2^{n-1} n!$

TABLE 3. The toroidal complexes.

In order to deal with tilings by finitely many simplices, and arguments motivating upcoming discussions of configuration spaces, we look at the quotient of the Euclidean space  $\mathbb{R}^n$  by the canonical group of translations, resulting in the  $n$ -torus  $\mathbb{T}^n$ . We call the quotient of the Coxeter complex  $\mathcal{C}W$  of Euclidean type as the *toroidal Coxeter complex*, denoted as  $\mathbb{T}\mathcal{C}W$ . Figure 2(a) shows the hyperplanes of  $\tilde{B}_2$  in  $\mathbb{R}^2$ , whereas (b) shows the hyperplanes for  $\tilde{A}_2$ . Figure 2(c) is the cellulation of the toroidal complex  $\mathbb{T}\mathcal{C}\tilde{A}_2$ .

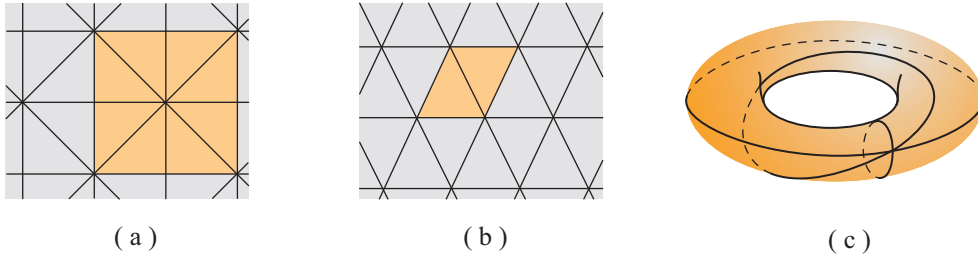


FIGURE 2. Coxeter complexes (a)  $\mathcal{C}\tilde{B}_2$ , (b)  $\mathcal{C}\tilde{A}_2$  and (c)  $\mathbb{T}\mathcal{C}\tilde{A}_2$ .

### 3. CONFIGURATION SPACES

3.1. There exists a configuration spaces of points associated to each Coxeter complex. We describe (quotients of) configuration spaces of particles on the line  $\mathbb{R}$  and the circle  $\mathbb{S}$  for the spherical and Euclidean cases. The constructions follow from the hyperplane arrangement of the reflection group.

**Definition 3.1.** Let  $C_n(\mathbb{R}) = \mathbb{R}^n - \{(x_1, x_2, \dots, x_n) \in \mathbb{R}^n \mid \exists i, j, x_i = x_j\}$  be the configuration space of  $n$  labeled particles on the real line  $\mathbb{R}$ . A generic point in  $C_5(\mathbb{R})$  is  $x_1 < x_2 < x_3 < x_4 < x_5$ , which we notate (without labels) as  $\circ - \circ - \circ - \circ - \circ$ .

**Definition 3.2.** Let  $C_{\bar{n}}(\mathbb{R}_{\bullet}) = \mathbb{R}^n - \{(x_1, x_2, \dots, x_n) \in \mathbb{R}^n \mid \exists i, j, x_i = \pm x_j \text{ or } x_i = 0\}$  be the space of  $n$  pairs of *symmetric* labeled particles (denoted  $\bar{n}$ ) across the origin. A point

in  $C_3(\mathbb{R}_\bullet)$  is  $-x_3 < -x_2 < -x_1 < 0 < x_1 < x_2 < x_3$ , which is depicted without labels as  $\circ-\circ-\circ-\bullet-\circ-\circ$ , where the black particle is fixed at the origin.

**Definition 3.3.** Let  $C_{\bar{n}}(\mathbb{R}_\circ) = \mathbb{R}^n - \{(x_1, x_2, \dots, x_n) \in \mathbb{R}^n \mid \exists i, j, x_i = \pm x_j\}$  be the space of  $\bar{n}$  pairs of symmetric labeled particles across the origin, where the particle  $x_i$  and its symmetric pair  $-x_i$  are both allowed to occupy the origin. A point in  $C_3(\mathbb{R}_\circ)$  is

$$(3.1) \quad -x_3 < -x_2 < -x_1 < x_1 < x_2 < x_3$$

drawn  $\circ-\circ-\circ-\mid-\circ-\circ$  without labels. Notice the mark at the origin where there is no fixed particle: The point  $-x_3 < -x_2 < x_1 < -x_1 < x_2 < x_3$  drawn as  $\circ-\circ-\circ-\mid-\circ-\circ$  lies in the same chamber of  $C_3(\mathbb{R}_\circ)$  as Eq.(3.1).

Let  $\text{Aff}(\mathbb{R})$  be the group of affine transformations of  $\mathbb{R}$  generated by translating and dilating. The action of  $\text{Aff}(\mathbb{R})$  on  $C_n(\mathbb{R})$  translates the leftmost of the  $n$  particles in  $\mathbb{R}$  to  $-1$  and the rightmost is dilated to 1. Taking the closure of this configuration space allows particles to *collide* (coincide with each other) on the line.

**Proposition 3.4.** *Let  $C_n(\mathbb{R})$  denote the closure of  $C_n(\mathbb{R})/\text{Aff}(\mathbb{R})$ . Then  $C_n(\mathbb{R})$  has the same cellulation as  $\mathcal{CA}_{n-1}$ .*

A detailed proof of this is given in [10, Section 4]. Roughly, quotienting by translations of  $\text{Aff}(\mathbb{R})$  removes the inessential component of the arrangement and dilating results in restricting to the sphere  $\mathcal{CA}_{n-1}$ .

The proposition above can be extended to the other spherical Coxeter complexes. Let  $\text{Aff}(\bar{\mathbb{R}})$  be the transformations of  $\mathbb{R}$  generated by dilating across the origin: The action of  $\text{Aff}(\bar{\mathbb{R}})$  dilates the (symmetric) particles farthest from the origin to unit distance. Let  $C_{\bar{n}}(\mathbb{R}_\bullet)$  and  $C_{\bar{n}}(\mathbb{R}_\circ)$  denote the closures of  $C_{\bar{n}}(\mathbb{R}_\bullet)/\text{Aff}(\bar{\mathbb{R}})$  and  $C_{\bar{n}}(\mathbb{R}_\circ)/\text{Aff}(\bar{\mathbb{R}})$  respectively.

**Theorem 3.5.**  *$C_{\bar{n}}(\mathbb{R}_\bullet)$  and  $C_{\bar{n}}(\mathbb{R}_\circ)$  have the same cellulation as  $\mathcal{CB}_n$  and  $\mathcal{CD}_n$  respectively.*

*Proof.* From the above definition above, it is clear  $C_{\bar{n}}(\mathbb{R}_\bullet)$  and  $C_{\bar{n}}(\mathbb{R}_\circ)$  are complements of the hyperplanes given in Table 2. The closure of the spaces simply include the hyperplanes back into  $\mathbb{R}^n$ . Thus any collision in the closed configuration space maps to a point on the hyperplanes defined by the associated finite reflection group. Quotienting by  $\text{Aff}(\bar{\mathbb{R}})$  allows choosing a particular representative for each fiber. Specifically, for the fiber containing  $(x_1, x_2, \dots, x_n)$ , choose

$$(x_1, x_2, \dots, x_n) / \sqrt{x_1^2 + x_2^2 + \dots + x_n^2},$$

giving a map onto the unit sphere in  $\mathbb{R}^n$ . The cellulation of the sphere by these hyperplanes yields the desired Coxeter complex.  $\square$

3.2. We move from the spherical to the affine (toroidal) complexes. However, the focus now is on configurations of particles on the circle  $\mathbb{S}$ . The group of rotations acts freely on  $C_{n+1}(\mathbb{S})$ , and its quotient  $C_n(\mathbb{S}^\bullet)$  simply fixes one of the  $n$  particles. Thus  $C_n(\mathbb{S}^\bullet)$  is the configuration space of  $n$  labeled particles on a circle with one fixed particle; Figure 3(a) shows a point in  $C_8(\mathbb{S}^\bullet)$  drawn without labels.

**Proposition 3.6.** *The closure  $C_n\langle\mathbb{S}^\bullet\rangle$  of  $C_n(\mathbb{S}^\bullet)$  has the same cellulation as  $\mathrm{TC}\tilde{A}_n$ .*

A proof of this is given in [9, Section 3]. A similar construction is produced for the other three toroidal Coxeter complexes. Our focus is on the circle  $\mathbb{S}$  with the vertical line through its center as its axis of symmetry, where the two diametrically opposite points on the axis are labeled 0 and 1. The space of interest is the configuration space of pairs of *symmetric* labeled particles (again denoted  $\bar{n}$ ) across this symmetric axis of the circle.

**Definition 3.7.** Let  $C_{\bar{n}}(\mathbb{S}_\circ^\bullet) = \mathbb{T}^n - \{(x_1, x_2, \dots, x_n) \in \mathbb{T}^n \mid \exists i, j, x_i = \pm x_j \text{ or } x_i = 1\}$  be the space of  $n$  pairs of symmetric labeled particles on  $\mathbb{S}$  with a fixed particle at 1. Figure 3(b) shows a point in  $C_5(\mathbb{S}_\circ^\bullet)$ .

**Definition 3.8.** Let  $C_{\bar{n}}(\mathbb{S}_\bullet^\circ) = \mathbb{T}^n - \{(x_1, x_2, \dots, x_n) \in \mathbb{T}^n \mid \exists i, j, x_i = \pm x_j \text{ or } x_i = 1 \text{ or } x_i = 0\}$  be the space of  $n$  pairs of symmetric labeled particles on  $\mathbb{S}$  with a fixed particle at 0 and 1. Figure 3(c) shows a point in  $C_5(\mathbb{S}_\bullet^\circ)$ .

**Definition 3.9.** Let  $C_{\bar{n}}(\mathbb{S}_\circ^\circ) = \mathbb{T}^n - \{(x_1, x_2, \dots, x_n) \in \mathbb{T}^n \mid \exists i, j, x_i = \pm x_j\}$  be the space of  $n$  pairs of symmetric labeled particles on  $\mathbb{S}$  with no fixed particles. Figure 3(d) shows a point in  $C_5(\mathbb{S}_\circ^\circ)$ .

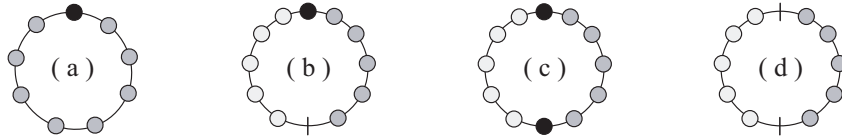


FIGURE 3. Configurations of particles (a) without and (b) - (d) with symmetry.

**Theorem 3.10.** *The closures  $C_{\bar{n}}\langle\mathbb{S}_\circ^\bullet\rangle$ ,  $C_{\bar{n}}\langle\mathbb{S}_\bullet^\circ\rangle$  and  $C_{\bar{n}}\langle\mathbb{S}_\circ^\circ\rangle$  have the same cellulation as  $\mathrm{TC}\tilde{B}_n$ ,  $\mathrm{TC}\tilde{C}_n$  and  $\mathrm{TC}\tilde{D}_n$  respectively.*

*Proof.* This is a direct consequence of the definitions of the configuration spaces, of the toroidal complexes, and their corresponding hyperplane arrangements given in Table 3.  $\square$

*Remark.* The group of reflections  $W$  across the respective hyperplanes act on the configuration space by permuting particles. In fact,  $W$  is the group of all possible permutations of the particles that preserve the structure of the configuration space (i.e., fixed particles remain fixed and symmetric pairs remain symmetric). That is,  $W$  has a transitive action on the chambers of  $\mathcal{C}W$ .

4. BRACKETINGS AND HYPERPLANES

4.1. We introduce the bracket notation in order to visualize collisions in the closed configuration spaces. A *bracket* is drawn around adjacent particles on a configuration space diagram representing the collision of the included particles. A *k-bracketing* of a diagram is a set of *k* brackets representing multiple independent particle collisions. For example, the configuration

$$(4.1) \quad -x_4 = -x_3 < -x_2 < -x_1 = 0 = x_1 < x_2 < x_3 = x_4$$

in  $C_5(\mathbb{R}_\bullet)$  corresponds to the bracketing . Each bracket on a configuration space diagram with symmetric particles will actually consist of two symmetric brackets, one on each side of the origin, with this symmetric pair counting as only one bracket. If this set includes the origin, we draw one symmetric bracket around the origin, which again counts as one bracket. Thus Eq.(4.1) is a 2-bracketing of its diagram.

We define the *support* of a bracketing to be the configuration space associated to the bracketing diagram; it is the subspace (of the configuration space) in which particles that share a bracket have collided. However, a set of collisions in a configuration space defines an intersection of hyperplanes. So, alternatively, the support of a bracketing is the smallest intersection of hyperplanes associated to the bracketing.

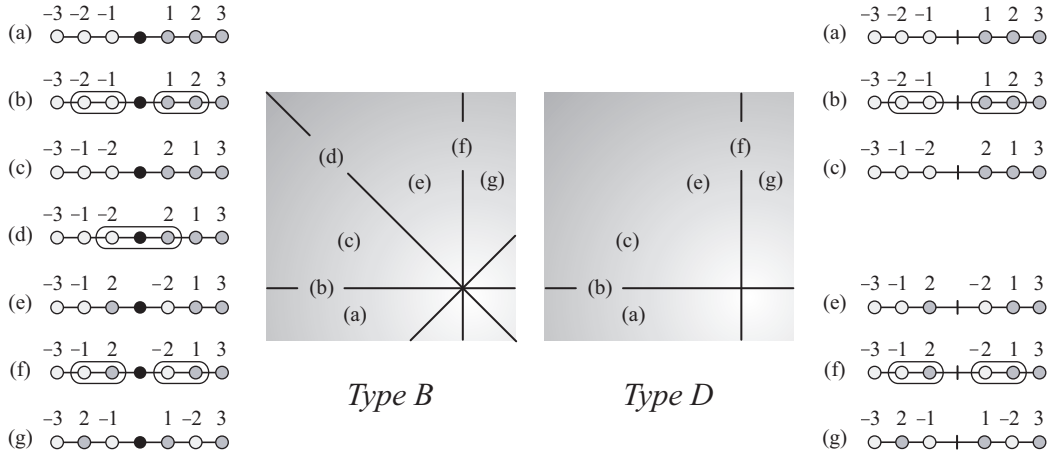


FIGURE 4. Local regions of  $CB_3$  and  $CD_3$ .

**Example 4.1.** Figure 4 shows part of the two-dimensional complexes  $CB_3$  and  $CD_3$ , one with a fixed particle at the axis of symmetry  $C_3(\mathbb{R}_\bullet)$  and one without  $C_3(\mathbb{R}_\circ)$ . As we move through the chambers, going from (a) through (g), a representative of each configuration is shown. Notice that since there is no fixed particle at the axis of symmetry for type *D*, there is no meaningful bracketing of the symmetric particles closest to the axis; they may pass each other freely *without* collision.

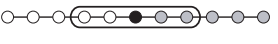
4.2. A set of hyperplanes of an algebraic variety  $V$  gives it a *cellulation*. Two cellulations are *isomorphic* if there is an isomorphism between the varieties that induces a bijection on the hyperplane sets. Let  $\alpha$  be an intersection of hyperplanes in a cellulation. We say that hyperplanes  $h_i$  *cellulate*  $\alpha$  to mean the intersections  $h_i \cap \alpha$  cellulate  $\alpha$ . Denote  $\mathcal{H}_s \alpha$  to be the set of all hyperplanes that contain  $\alpha$ . If reflections in these hyperplanes generate a finite reflection group, it is called the *stabilizer* of  $\alpha$ . Note that in a Coxeter complex, the stabilizer exists for all intersections of hyperplanes.<sup>1</sup>

Let  $G$  be a  $k$ -bracketing diagram and let  $\alpha$  be the support of  $G$ . Determining the stabilizing hyperplanes of  $\alpha$  follows from the following lemma, which comes straight from the definition.

**Lemma 4.2.** *If  $\alpha$  is the support of a bracketing  $G$ , then for every pair of particles  $x_i$  and  $x_j$  that share a bracket in  $G$ , the hyperplane defined by  $x_i = x_j$  is in  $\mathcal{H}_s \alpha$ .*

The hyperplanes of the cellulation of  $\alpha$  represent all possible collisions of pairs of particles in that configuration space. However, many collisions are redundant and represent the same set of configurations. Other collisions, such as those between particles that share a bracket, occur at all configurations in  $\alpha$  and do not define a hyperplane properly contained in  $\alpha$ . We formalize this idea:

**Lemma 4.3.** *If  $\alpha$  is the support of a bracketing  $G$ , then the cellulation of  $\alpha$  is the configuration space of a diagram  $G_0$ , which is obtained from  $G$  by replacing each bracket with a particle.*

**Example 4.4.** Let  $\alpha$  be the intersection of hyperplanes  $x_1 = x_2 = 0$  in  $\mathcal{CB}_5$ . Its diagram looks similar to . The hyperplanes that cellulate  $\alpha$  are all of the hyperplanes of  $\mathcal{CB}_5$ ; however, collisions between  $x_1$  and  $x_2$  are irrelevant to the cellulation (since they are part of the defining hyperplanes of  $\alpha$ ). Furthermore no particle can collide with  $x_1$  or  $x_2$  without also colliding with the fixed particle 0. Thus the remaining hyperplanes, after the redundant ones are removed, are  $x_i = x_j$ ,  $x_i = -x_j$ , and  $x_i = 0$  for all  $i, j > 2$ . Thus  $\alpha$  is cellulated by the  $B_3$  hyperplane arrangement.

4.3. There are natural composition maps on configuration space diagrams that encode the cellulation and stabilizer of a given subspace.

**Definition 4.5.** There are two types of compositions:

1. Let  $G_0$  be a diagram of  $m$  (possibly paired) particles of a configuration space with one particle labeled  $i$ . Let  $G_1$  be a diagram of  $C_k(\mathbb{R})$ . The *composition*  $G_0 \circ_i G_1$  is the diagram of  $m + k - 1$  (possibly paired) particles where the particle  $i$  is replaced by a bracket containing  $G_1$  (left side of Figure 5).

<sup>1</sup>By abuse of terminology, we also refer to the set  $\mathcal{H}_s \alpha$  as the stabilizer of  $\alpha$ .

2. Let  $G_0$  be a diagram of a  $C_m(\mathbb{R}_\bullet)$  with the fixed particle labeled  $i$ , and let  $G_1$  be a diagram of either  $C_k(\mathbb{R}_\bullet)$  or  $C_k(\mathbb{R}_\circ)$ . The *composition*  $G_0 \circ_i G_1$  is the diagram of  $m+k$  paired particles where the particle  $i$  is replaced by a bracket containing  $G_1$  (right side of Figure 5).

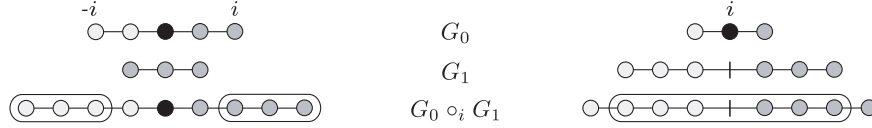


FIGURE 5. Composition operations on bracketings.

Indeed any  $k$ -bracketing  $G$  can be represented as

$$(4.2) \quad G_0 \circ_{i_1} G_1 \circ_{i_2} \cdots \circ_{i_k} G_k,$$

where each  $G_i$  is a diagram without brackets and  $i_j$  is a particle in  $G_0$ . From this terminology, the following is a consequence of Lemmas 4.2 and 4.3.

**Proposition 4.6.** *Let  $G$  be a  $k$ -bracketing as defined in Eq.(4.2) and let  $\alpha$  be its support. Then the cellulation of  $\alpha$  is determined by  $G_0$  and the stabilizer of  $\alpha$  is the product of the configuration spaces diagramed by  $G_1, G_2, \dots, G_k$ .*

Each valid ordering of particles on the configuration space diagram corresponds to a chamber. We define the *symmetric action*  $\sigma(G)$  on a diagram  $G$  as follows: For a diagram  $G$  with no brackets, the elements of  $\sigma$  correspond to all valid reorderings of the particles of  $G$ . Thus each element of  $\sigma(G)$  takes  $G$  to a diagram of a different chamber, and each chamber of the configuration space is in the image  $\sigma(G)$ .<sup>2</sup> In the case of bracketings, define  $\sigma(G)$  to be the set of permutations of particles which preserve the bracketing; that is, only those reorderings in which the sets of particles sharing a bracket remain unchanged. Thus  $\sigma(G)$  acts independently on each bracket and on the base space  $G_0$  and

$$\sigma(G) = \sigma(G_0) \times \sigma(G_1) \times \cdots \times \sigma(G_k).$$

Geometrically, particles sharing a bracket have already collided. Reordering particles within a bracket has no impact on the configurations represented by  $G$ . Thus all bracketings in the image of

$$\sigma(G_1) \times \cdots \times \sigma(G_k)$$

correspond to the same cell in the support of  $G$ . This amounts to a gluing rule for the tiling of the configuration space: Two faces of different chambers are identified if their bracketings correspond to the same cell.

<sup>2</sup>Thus the support of  $G$  is the set of configurations represented by the bracketings in the image of  $\sigma(G)$ .

4.4. It is easy to check that in most cases the cellulations of Coxeter complexes are indeed other (smaller dimensional) Coxeter complexes. There are, however, three instances where subspaces (intersections of hyperplanes) of the Coxeter complexes  $\mathcal{CD}_n$ ,  $\mathbb{TC}\tilde{\mathcal{B}}_n$  and  $\mathbb{TC}\tilde{\mathcal{D}}_n$  are not Coxeter complexes themselves. In particular, these subspaces have cellulations combinatorially equivalent to a Coxeter complexes with *additional* hyperplanes. We define these three atypical complexes below:

**Definition 4.7.** The complexes of interest are:

1. Let  $\mathcal{CD}_{n,m}$  be  $\mathcal{CD}_n$  with  $m$  additional hyperplanes  $\{x_i = 0 \mid 1 \leq i \leq m\}$ .
2. Let  $\mathbb{TC}\tilde{\mathcal{B}}_{n,m}$  be  $\mathbb{TC}\tilde{\mathcal{B}}_n$  with  $m$  additional hyperplanes  $\{x_i = 0 \mid 1 \leq i \leq m\}$ .
3. Let  $\mathbb{TC}\tilde{\mathcal{D}}_{n,m}$  be  $\mathbb{TC}\tilde{\mathcal{D}}_n$  with  $2m$  additional hyperplanes  $\{x_i = 0, x_i = 1 \mid 1 \leq i \leq m\}$ .

The configuration space model provides intuition into how these cases arise naturally. Note how these are all complexes with associated configuration spaces on  $\mathbb{R}_\circ$ ,  $\mathbb{S}_\circ^\bullet$  and  $\mathbb{S}_\circ^\circ$ , where not all points along the axis of symmetry have fixed particles. The subspaces of these configuration spaces are those where some particles have collided. In these subspaces, sets of collided particles may be considered in aggregate as a new type of particle, called a *thick* particle. Figure 6(a) shows a bracketing and (b) its representation with thick particles. In general, thick particles allow us to represent any number of coincident particles by a single particle.

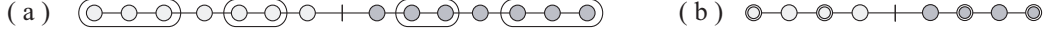


FIGURE 6. Bracketing and thick points.

Recall that particles were defined such that they could occupy the same point as their inverse; that is, they do not form a collision with their inverse. Unlike (standard) particles, a thick particle and its inverse may not occupy the same point on the manifold, and thus can collide. Note that the number  $m$  of additional hyperplanes added to the complex corresponds to the number  $m$  of thick particles in their configuration spaces. Then the diagram of Figure 6(b) is an element of  $\mathcal{CD}_{4,2}$ , sitting as a subspace of  $\mathcal{CD}_7$  in Figure 6(a).

*Remark.* In the case of non-paired particles, the distinction between standard and thick particles is irrelevant, since no particle has an inverse to collide with. They are also inconsequential in configuration spaces that include a fixed particle at every point where particles may meet their inverses.

## 5. A COMPACTIFICATION

5.1. The collection of hyperplanes  $\{x_i = 0 \mid i = 1, \dots, n\}$  of  $\mathbb{R}^n$  generates the *coordinate* arrangement. A crossing of hyperplanes is *normal* if it is locally isomorphic to a coordinate arrangement. A construction which transforms any crossing into a normal crossing involves the algebro-geometric concept of a blow-up.

**Definition 5.1.** The *blow-up* of a variety  $V$  along a codimension  $k$  intersection  $\alpha$  of hyperplanes is the closure of  $\{(x, f(x)) \mid x \in V\}$  in  $V \times \mathbb{P}^{k-1}$ . The function  $f : V \rightarrow \mathbb{P}^{k-1}$  is defined by  $f : p \mapsto [f_1(p) : f_2(p) : \cdots : f_k(p)]$ , where the  $f_i$  define hyperplanes of  $\mathcal{H}_s\alpha$  whose intersection is  $\alpha$ .

We denote the blow-up of  $V$  along  $\alpha$  by  $V_{\# \alpha}$ . There is a natural projection map

$$\pi : V_{\# \alpha} \rightarrow V : (x, y) \mapsto x$$

which is an isomorphism on  $V - \alpha$ . The hyperplanes of  $V_{\# \alpha}$  are the closures  $\pi^{-1}(h - \alpha)$  for each hyperplane  $h$  of  $V$  and one additional hyperplane  $\pi^{-1}(\alpha)$ . Thus  $V - \alpha$  and  $V_{\# \alpha} - \pi^{-1}(\alpha)$  are isomorphic not only as varieties but as cellulations. The hyperplane  $\alpha$  of  $V_{\# \alpha}$  has a natural identification with the projectified normal bundle of  $\alpha$  in  $V$ .

A general collection of blow-ups is usually noncommutative in nature; in other words, the order in which spaces are blown up is important. For a given arrangement, De Concini and Procesi [7] establish the existence (and uniqueness) of a *minimal building set*, a collection of subspaces for which blow-ups commute for a given dimension, and for which every crossing in the resulting space is normal. For a Coxeter complex  $\mathcal{C}W$ , we denote the minimal building set by  $\text{Min}(\mathcal{C}W)$ .

**Definition 5.2.** The cellulation  $\mathcal{C}(W)_{\#}$  is the *minimal blow-up* of  $\mathcal{C}W$ , obtained by blowing up along elements of  $\text{Min}(\mathcal{C}W)$  in *increasing* order of dimension.

**Example 5.3.** Figure 7(a) shows the blow-ups of the sphere  $\mathcal{C}A_3$  of Figure 1(a) at nonnormal crossings. Each blown up point has become a hexagon with antipodal identification and the resulting manifold is  $\mathcal{C}(A_3)_{\#}$ , homeomorphic to  $\#^8 \mathbb{R}P^2$ . Figure 7(b) shows the minimal blow-up of  $\tilde{\mathcal{C}}A_2$  of Figure 2(c).

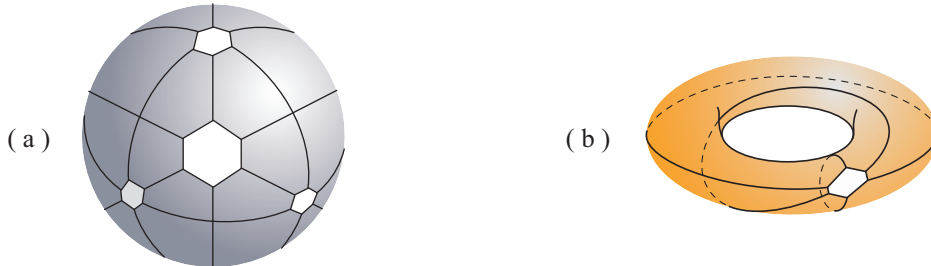


FIGURE 7. Minimal blow-up of the complexes (a)  $\mathcal{C}A_3$  and (b)  $\tilde{\mathcal{T}}A_2$ .

*Remark.* Kapranov noticed that  $\mathcal{C}(A_n)_{\#}$  is isomorphic to  $\overline{\mathcal{M}}_0^{n+2}(\mathbb{R})$ , the real points of the Deligne-Knudsen-Mumford compactification of the moduli space of Riemann spheres with marked punctures [12]. A combinatorial proof of this is given in [10].

5.2. The relationship between the set  $\text{Min}(CW)$  and the group  $W$  is given by the concept of reducibility.

**Definition 5.4.** For intersections of hyperplanes  $\alpha, \beta$ , and  $\gamma$ , the collection of hyperplanes  $\mathcal{H}_s\alpha$  is *reducible* if  $\mathcal{H}_s\alpha$  is a disjoint union  $\mathcal{H}_s\beta \sqcup \mathcal{H}_s\gamma$ , where  $\alpha = \beta \cap \gamma$ .

**Lemma 5.5.** [5] *Let  $\alpha$  be an intersection of hyperplanes of  $CW$ . Then  $\mathcal{H}_s\alpha$  is irreducible if and only if  $\alpha \in \text{Min}(CW)$ .*

The lemma above can be rewritten in the language of bracketings.

**Lemma 5.6.** *Let  $\alpha$  be an intersection of hyperplanes of  $CW$ . Then  $\alpha \in \text{Min}(CW)$  if and only if  $\alpha$  is the support of a 1-bracketing.*

*Proof.* If  $\alpha$  is the support of a 1-bracketing  $G$ , then  $\mathcal{H}_s\alpha$  is determined again by Lemma 4.2. As a result:

- (1) If  $g$  contains a fixed particle, then  $\mathcal{H}_s\alpha \cong \mathcal{H}B_k$ .
- (2) If  $g$  contains a particle and its inverse but no fixed particle, then  $\mathcal{H}_s\alpha \cong \mathcal{H}D_k$ .
- (3) If  $g$  does not contain a particle and its inverse, then  $\mathcal{H}_s\alpha \cong \mathcal{H}A_k$ .

All three of these hyperplane arrangements are irreducible, so  $a \in \text{Min}(CW)$ .

Conversely, let  $\alpha$  be the support of a  $k$ -bracketing  $G = G_0 \circ_{i_1} G_1 \circ_{i_2} \cdots \circ_{i_k} G_k$ . Let  $\beta$  be the support of  $G_1$  and  $\gamma$  be the product of the configuration spaces diagramed by  $G_2, \dots, G_k$ . By the definition of reducibility,  $\mathcal{H}_s\alpha = \mathcal{H}_s\beta \sqcup \mathcal{H}_s\gamma$ , and thus  $a \notin \text{Min}(CW)$  by Lemma 5.5.  $\square$

Using Proposition 4.6, Table 5 itemizes the collection for the spherical cases and Table 6 for the Euclidean ones. In the tables,  $m$  represents the total number of thick particles and  $r$  the number of thick particles in the bracket (stabilizer) of the atypical complexes of Definition 4.7.

5.3. Compactifying a configuration space  $C_n(M)$  enables the points on  $M$  to collide and a *system* is introduced to record the *directions* points arrive at the collision. In the work of Fulton and MacPherson [11], this method is brought to rigor in the algebro-geometric context. As mentioned above, for an arrangement of hyperplanes, De Concini and Procesi develop a method to compactify their complements by iterated blow-ups using a minimal building set. In the case of the arrangement  $M^n - C_n(M)$ , their procedure yields the Fulton-MacPherson compactification of  $C_n(M)$  [7]. Thus, the minimal blow-ups of the Coxeter complexes  $CW$  are equivalent to the Fulton-MacPherson compactifications of their corresponding configuration spaces.

As bracketing encoded faces of closed configuration spaces, *nested* bracketings keep track of compactified configuration spaces [7, Section 2]. The Fulton-MacPherson compactification encodes additional information about how collisions have occurred, viewing it as the

order in which the particles collide: When a bracketing  $G_1$  is nested in  $G_2$ , it represents configurations in which the particles of  $G_1$  collided with each other before they collided with rest of the particles of  $G_2$ . Indeed, the codimension  $k$  faces of a chamber of a compactified configuration space are the nested  $k$ -bracketings on the configuration space diagrams.

A diagram  $G$  defined as

$$(5.1) \quad G_0 \circ_{i_1} G_1 \circ_{i_2} \cdots \circ_{i_k} G_k,$$

is a nested  $(k + m_0 + m_1 + \cdots + m_k)$ -bracketing, where  $i_j$  is a particle in  $G_0$  and where  $G_i$  is a nested  $m_i$ -bracketing. Figure 8 shows an example.

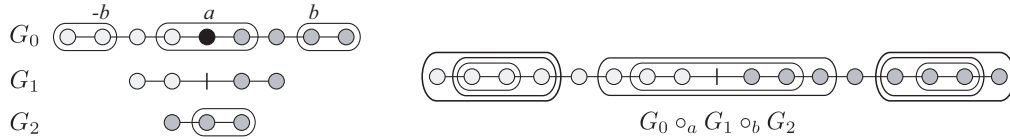


FIGURE 8. Composition operations on nested bracketings.

As before, the support of a nested  $k$ -bracketing  $G$  is the smallest intersection of hyperplanes containing the configurations represented by  $G$ . It is the subspace in which the collisions represented by  $G$  have not only occurred, but have occurred in the order implied by the nesting of brackets in  $G$ . The set of configurations in the support is represented by all reorderings of particles that preserve the bracketing.

**Theorem 5.7.** *Given a nested bracketing  $G$  in a compactified configuration space, the support of  $G$  contains configurations represented by the images of  $G$  under  $\sigma(G)$ .*

*Proof.* From Lemma 5.6, the hyperplanes of  $\mathcal{C}(W)_\#$  correspond to the supports of 1-bracketings. Thus the hyperplanes containing the configurations represented by  $G$  are the hyperplanes corresponding to the brackets in  $G$ . Therefore the support of  $G$  consists of all orderings of particles that respect the brackets of  $G$ . By definition,  $\sigma(G)$  performs these reorderings.  $\square$

After compactification, different orderings of particles in a bracket do not necessarily represent the same cell. A different action is necessary to describe the identification of diagrams of a projective screen.

**Definition 5.8.** The *twisting*  $\hat{\sigma}(G)$  action on a unbracketed diagram  $G$  has the identity and the reflection (that reverses the order of the particles of  $G$ ). On a nested bracketing diagram, the action of  $\hat{\sigma}(G)$  acts independently on each component.

**Theorem 5.9.** *Let  $G$  be a nested bracketing in a compactified configuration space, as defined in Eq.(5.1). All bracketings in the image of  $G$  under  $\hat{\sigma}(G_1) \times \hat{\sigma}(G_2) \times \cdots \times \hat{\sigma}(G_k)$  represent the same cell.*

*Proof.* By definition, blow-ups introduce a *projective* bundle around each subspace in the minimal building set. The analog in configuration spaces is an identification in each bracket: Reversing the positions of the particles in the bracket is defined to represent the same configuration. Thus the permutations that represent the same set of configurations as  $G$  are exactly the images of  $G$  under  $\hat{\sigma}(G_1) \times \hat{\sigma}(G_2) \times \cdots \times \hat{\sigma}(G_k)$ .  $\square$

*Remark.* This theorem gives us a gluing rule between the faces of two chambers. In other words, two nested  $k$ -bracketings  $G_1$  and  $G_2$  of a diagram (representing codimension  $k$ -faces) are identified if  $G_2$  can be obtained from  $G_1$  by twisting some of the brackets of  $G_2$ .

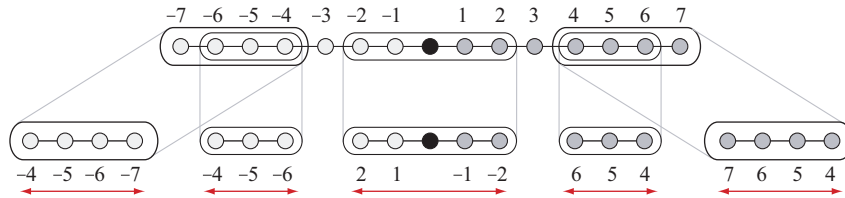


FIGURE 9. Twisting on nested bracketings.

Figure 9 shows the permutations that preserve the cell represented by a particular configuration space diagram. Note that reflections permute with each other, and thus they generate a group which is isomorphic to  $(\mathbb{Z}/2\mathbb{Z})^3$ .

Combining the previous two theorems, we can define an action on the support  $\alpha$  of  $G$  which is faithful on the chambers of  $\alpha$ . Thus we can express the cellulation of  $\alpha$  in terms of a set of equivalence classes of  $\sigma(G)$ .

**Corollary 5.10.** *The action of  $\sigma_G/(\hat{\sigma}_{G_1} \times \hat{\sigma}_{G_2} \times \cdots \times \hat{\sigma}_{G_k})$  permutes the chambers of  $\alpha$ ; only the identity acts trivially.*

5.4. Classically, the notion of an operad was created for the study of iterated loop spaces. Since then, operads have been used as universal objects representing a wide range of algebraic concepts. We give a brief definition.

**Definition 5.11.** An *operad*  $\{\mathcal{O}(n) \mid n \in \mathbb{N}\}$  is a collection of objects  $\mathcal{O}(n)$  in a monoidal category endowed with certain extra structures, notably  $\mathcal{O}(n)$  carries an action of the symmetric group of  $n$  letters, and there are composition maps

$$\mathcal{O}(n) \otimes \mathcal{O}(k_1) \otimes \cdots \otimes \mathcal{O}(k_n) \rightarrow \mathcal{O}(k_1 + \cdots + k_n)$$

which satisfy certain axioms, cf. [13].

The nested bracketings, along with the composition map of Eq.(5.1), of diagrams in  $C_n(\mathbb{R})$  leads to an  $A_\infty$  operad structure [14], and of diagrams in  $C_n(\mathbb{S}^\bullet)$  to a module over an operad structure [13]. It is important to note that the symmetric group, which acts on  $\mathcal{O}(n)$ ,

is exactly the type  $A$  Coxeter group. Moreover, the bracketings for all the configuration spaces discussed here carry a natural action of their associated Coxeter group  $W$ .

6. TILING BY GRAPH-ASSOCIAHEDRA

6.1. It is a classic result of geometric group theory that each chamber of a Coxeter complex is a simplex [3, §1]. However, we are interested in the minimal blow-ups of these manifolds.

**Definition 6.1.** Let  $\Gamma$  be a graph. A *tube* is a proper nonempty set of nodes of  $\Gamma$  whose induced graph is a proper, connected subgraph of  $\Gamma$ . There are three ways that two tubes  $t_1$  and  $t_2$  may interact on the graph.

- (1) Tubes are *nested* if  $t_1 \subset t_2$ .
- (2) Tubes *intersect* if  $t_1 \cap t_2 \neq \emptyset$  and  $t_1 \not\subset t_2$  and  $t_2 \not\subset t_1$ .
- (3) Tubes are *adjacent* if  $t_1 \cap t_2 = \emptyset$  and  $t_1 \cup t_2$  is a tube in  $\Gamma$ .

Tubes are *compatible* if they do not intersect and they are not adjacent. A *tubing*  $T$  of  $\Gamma$  is a set of tubes of  $\Gamma$  such that every pair of tubes in  $T$  is compatible. A *k-tubing* is a tubing with  $k$  tubes.

**Definition 6.2.** For a given graph  $\Gamma$  with  $n$  nodes, the *graph-associahedron*  $\mathcal{P}\Gamma$  is the convex polytope of dimension  $n - 1$  whose face poset is isomorphic to set of valid tubings of  $\Gamma$ , ordered such that  $T \prec T'$  if  $T$  is obtained from  $T'$  by adding tubes.

Figure 10 shows two examples of graph-associahedra, having underlying graphs as paths and cycles, respectively, with three nodes. These turn out to be the two-dimensional associahedron [14] and cyclohedron [1] polytopes.

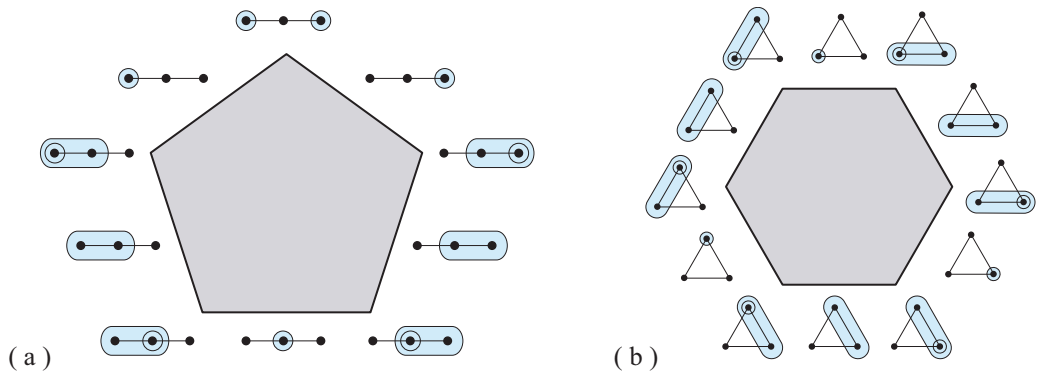


FIGURE 10. Graph-associahedra with (a) path and (b) cycle as underlying graphs.

**Theorem 6.3.** [4, Section 4] *Let  $W$  be a simplicial Coxeter group and  $\Gamma_W$  be its associated Coxeter graph. Then  $\mathcal{P}\Gamma_W$  is the fundamental domain for  $CW_{\#}$ .*

*Notation.* We write  $\mathcal{PW}$  instead of  $\mathcal{P}\Gamma_W$  when context makes it clear.

**Proposition 6.4.** *The tiling of the Coxeter cellulations are given as follows:*

- (1)  $\mathcal{P}A_n$  (the associahedron) tiles  $\mathcal{C}(A_n)_\#$ ,  $\mathcal{C}(B_n)_\#$  and  $\mathbb{TC}(\tilde{C}_n)_\#$ .
- (2)  $\mathcal{P}\tilde{A}_n$  (the cyclohedron) tiles  $\mathbb{TC}(\tilde{A}_n)_\#$ .
- (3)  $\mathcal{P}D_n$  tiles  $\mathcal{C}(D_n)_\#$  and  $\mathbb{TC}(\tilde{B}_n)_\#$ .
- (4)  $\mathcal{P}\tilde{D}_n$  tiles  $\mathbb{TC}(\tilde{D}_n)_\#$ .

*Proof.* For a given graph  $\Gamma$ , the polytope  $\mathcal{P}\Gamma_n$  depends only on the adjacency of nodes, not the label on the edges. □

*Remark.* There is a natural bijection from the set of all bracketings of a configuration space diagram to the set of all tubings of the associated Coxeter diagram. The bijection is such that two brackets intersect if and only if their images intersect or are adjacent as tubes. Thus the face poset of tubings is isomorphic to the face poset of bracketings, where  $k$  brackets correspond to a codimension  $k$  face. Figure 11 shows some examples of this bijection.

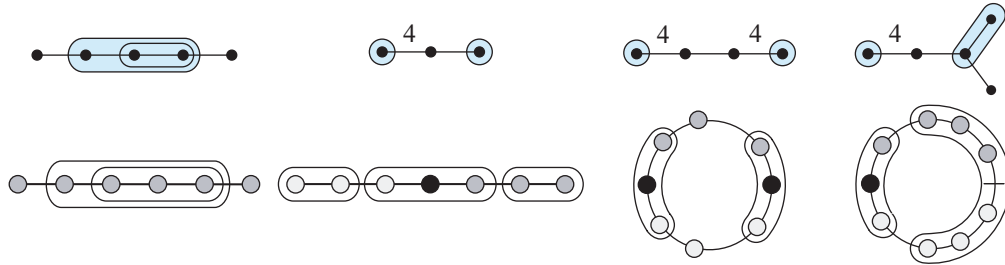


FIGURE 11. Examples of the bijection between tubings and nested bracketings.

6.2. We analyze the structure of these tiling polyhedra  $\mathcal{PW}$ . For a given tube  $t$  and a graph  $\Gamma$ , let  $\Gamma_t$  denote the induced subgraph on the graph  $\Gamma$ . By abuse of notation, we sometimes refer to  $\Gamma_t$  as a tube.

**Definition 6.5.** Given a graph  $\Gamma$  and a tube  $t$ , construct a new graph  $\Gamma_t^*$  called the *reconnected complement*: If  $V$  is the set of nodes of  $\Gamma$ , then  $V - t$  is the set of nodes of  $\Gamma_t^*$ . There is an edge between nodes  $a$  and  $b$  in  $\Gamma_t^*$  if either  $\{a, b\}$  or  $\{a, b\} \cup t$  is connected in  $\Gamma$ .

**Theorem 6.6.** [4, Section 3] *The facets of  $\mathcal{P}\Gamma$  correspond to the set of 1-tubings on  $\Gamma$ . In particular, the facet associated to a 1-tubing  $\{t\}$  is equivalent to  $\mathcal{P}\Gamma_t \times \mathcal{P}\Gamma_t^*$ .*

The facets of  $\mathcal{PW}$  are of the form  $\mathcal{P}\Gamma \times \mathcal{P}\Gamma^*$ , which can be found by simple inspection. Using induction of each term of the product produces the following results:

**Corollary 6.7.** *The faces of  $\mathcal{P}A$  are of the form  $\mathcal{P}A \times \cdots \times \mathcal{P}A$ .*

**Corollary 6.8.** *The faces of  $\mathcal{P}\tilde{A}$  are of the form  $\mathcal{P}\tilde{A} \times \mathcal{P}A \times \cdots \times \mathcal{P}A$ .*

Before moving on to the other tiling polytopes, we need to look at some special graphs which appear as reconnected complements. They are displayed in the third column of Table 1, the subscript  $n$  denoting the number of vertices. Note that the polytope  $\mathcal{P}X_4$  is the 3-dimensional *permutohedron*.

**Corollary 6.9.** *The faces of  $\mathcal{P}D$  are of the form*

- (1)  $\mathcal{P}A \times \cdots \times \mathcal{P}A$
- (2)  $\mathcal{P}D \times \mathcal{P}A \times \cdots \times \mathcal{P}A$
- (3)  $\mathcal{P}X^a \times \mathcal{P}A \times \cdots \times \mathcal{P}A$ .

**Example 6.10.** Figure 12 illustrates four different polyhedra. The first three are well-known objects: (a) the associahedron  $\mathcal{P}A_4$ , (b) cyclohedron  $\mathcal{P}\tilde{A}_4$  and (c) permutohedron  $\mathcal{P}X_4$ . The last one (d) is  $\mathcal{P}D_4$  with six pentagons  $\mathcal{P}A_3$ , three squares  $\mathcal{P}D_2 \times \mathcal{P}A_2$  and one hexagon  $\mathcal{P}X_3^a$  for facets.

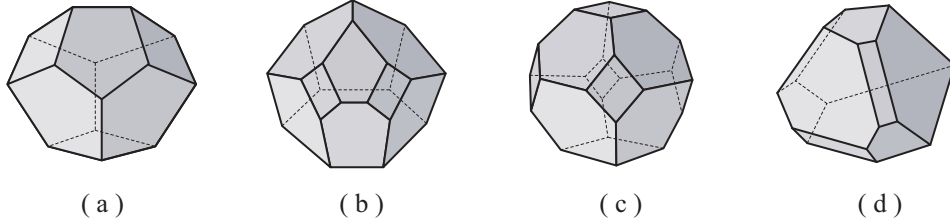


FIGURE 12. The 3-dimensional (a) associahedron  $\mathcal{P}A_4$ , (b) cyclohedron  $\mathcal{P}\tilde{A}_4$ , (c) permutohedron  $\mathcal{P}X_4$  and (d)  $\mathcal{P}D_4$ .

**Corollary 6.11.** *The faces of  $\mathcal{P}\tilde{D}$  are of the form*

- |  |  |
|--|--|
| (1) $\mathcal{P}A \times \cdots \times \mathcal{P}A$   | (6) $\mathcal{P}D \times \mathcal{P}D \times \mathcal{P}A \times \cdots \times \mathcal{P}A$ |
| (2) $\mathcal{P}D \times \mathcal{P}A \times \cdots \times \mathcal{P}A$                         | (7) $\mathcal{P}X^b \times \mathcal{P}A \times \cdots \times \mathcal{P}A$                   |
| (3) $\mathcal{P}X^a \times \mathcal{P}A \times \cdots \times \mathcal{P}A$                       | (8) $\mathcal{P}X^c \times \mathcal{P}A \times \cdots \times \mathcal{P}A$                   |
| (4) $\mathcal{P}X^a \times \mathcal{P}X^a \times \mathcal{P}A \times \cdots \times \mathcal{P}A$ | (9) $\mathcal{P}\tilde{D} \times \mathcal{P}A \times \cdots \times \mathcal{P}A$             |
| (5) $\mathcal{P}D \times \mathcal{P}X^a \times \mathcal{P}A \times \cdots \times \mathcal{P}A$   | (10) $\mathcal{P}X_4 \times \mathcal{P}A \times \cdots \times \mathcal{P}A$ .                |

6.3. We exhibit an algorithm that allows us to compute the Euler characteristic of the blown-up Coxeter complexes. From Theorem 6.6, we see that the number of codimension  $k$  faces of the polytope  $\mathcal{P}W$  cellulating  $\mathcal{C}W_\#$  is precisely the number of  $k$ -tubings of the associated Coxeter diagram  $\Gamma_W$ .

**Theorem 6.12.** *Let  $f_k$  be the number of  $k$ -dimensional faces of  $\mathcal{P}W$ , and let  $g$  be the number of chambers in the spherical or toroidal Coxeter complex  $CW$ . Then*

$$\chi(\mathcal{C}(W)_\#) = \sum_{k=0}^{n-1} (-1)^k \frac{g \cdot f_k}{2^{n-k}}.$$

*Proof.* Since all the crossings in  $\mathcal{C}(W)_\#$  are normal, each codimension  $k$  face of  $\mathcal{P}W$  is identified with  $2^k$  copies. □

Thus calculating the Euler characteristic amounts to finding the number of  $k$ -tubings  $f_k$  on a given diagram. We thank B. DeMedeiros [8] for motivating the idea to determine them. In the algorithm, given in Table 7,  $p_i$  will always denote a prime number, with  $p_i \neq p_j$  if  $i \neq j$  (the subscripts being compared as strings). The input is a graph  $G = (V, E)$  with  $V = \{v_1, \dots, v_n\}$  and a positive integer  $k$ ; the output is the number of  $k$ -tubings of  $G$ .

The general idea is to assign to each node a unique number such that the assignments reflect the adjacency relations in the graph. More precisely, the numbers associated to two nodes are relatively prime if and only if they are not adjacent (lines 1 - 5). A  $k$ -tubing will then correspond to a  $k$ -tuple of numbers, with each tube in the tubing consisting of all nodes whose numbers divide a particular element of the  $k$ -tuple. The test in line 8 ensures that the numbers of the  $k$ -tuple are such that proper nesting rules are satisfied, and lines 10 - 20 ensure that the tubes are connected (i.e., that they surround a connected subgraph of  $G$ ). From these facts it should be clear that the algorithm outputs the correct number. Some values of  $\chi(\mathcal{C})$ , for various complexes, are listed in Table 8.

6.4. The polytopes tiling the minimal blow-ups of the Coxeter complexes are given by Proposition 6.4. We now discuss the tiling of the atypical complexes, given in Definition 4.7, after minimal blow-ups. As in other (compactified) configuration spaces, the chambers of these complexes correspond to orderings of the particles. However, different orderings of particles may give different face posets to the chamber, since switching a standard and thick particle may change the valid bracketings of the diagram. Specifically, near an axis of symmetry with no fixed particles, having thick particles allows more collisions and hence more brackets, than having standard particles. It is here where the polytopes  $\mathcal{P}X^a$ ,  $\mathcal{P}X^b$ , and  $\mathcal{P}X^c$  based on Table 1 appear.

Recall that the chambers of these complexes arise as subspaces of  $\mathcal{C}(D_n)_\#$ ,  $\mathbb{TC}(\tilde{B}_n)_\#$  or  $\mathbb{TC}(\tilde{D}_n)_\#$ . From Proposition 6.4, these chambers must be *faces* of either  $\mathcal{P}D$  or  $\mathcal{P}\tilde{D}$ . Converting bracketings to tubings allows us to compute the face poset of the chamber using Theorem 6.6. The following is an example of this method. Table 4 lists the number of each type of polytope cellulating the corresponding atypical complexes. Note how there is not simply one type of polytope tiling each blown-up atypical complex, as was the case with the Coxeter complexes.

	$\mathcal{C}(D_{n+1,k})_{\#}$	$\mathbb{T}\mathcal{C}(\tilde{B}_{n,k})_{\#}$	$\mathbb{T}\mathcal{C}(\tilde{D}_{n,k})_{\#}$
$\mathcal{P}B_{n+1}$	$n! 2^{n+1} k$	$(n-1)! 2^n k$	$(n-k)! k! 2^n \binom{n-2}{k-2}$
$\mathcal{P}D_{n+1}$	$(n-1)! 2^{n+1} \binom{n-k+1}{2}$	$(n-2)! 2^n \binom{n-k}{2}$	$(n-k)! k! 2^n \binom{n-3}{k-1}$
$\mathcal{P}\tilde{D}_{n+1}$	0	0	$(n-k)! k! 2^{n-2} \binom{n-4}{k}$
$\mathcal{P}X_{n+1}^a$	$(n-1)! 2^n k$	$(n-2)! 2^{n-1} k$	$(n-k)! k! 2^n \binom{n-3}{k-2}$
$\mathcal{P}X_{n+1}^b$	0	0	$(n-k)! k! 2^{n-1} \binom{n-4}{k-1}$
$\mathcal{P}X_{n+1}^c$	0	0	$(n-k)! k! 2^{n-2} \binom{n-4}{k-2}$

TABLE 4. Enumeration of polytope tiles of the blown-up atypical complexes.

**Example 6.13.** By taking different bracketings in configurations  $C_5(\mathbb{R}_o)$  associated to  $\mathcal{C}(D_5)_{\#}$ , we can produce the configuration space diagrams of different chambers of  $\mathcal{C}(D_{4,1})_{\#}$ , as in Figure 13. By converting bracketings to tubings using the bijection, each facet of the chamber corresponds to the appropriate reconnected complement.

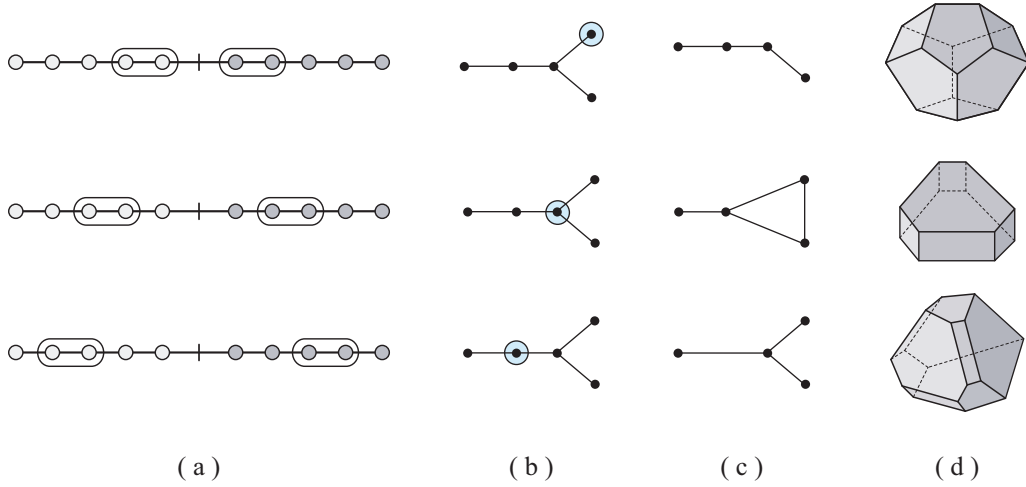


FIGURE 13. (a) Configuration diagram brackets, (b) associated tubing, (c) reconnected complements and (d) fundamental chambers.

The gluing rules for the compactified configuration spaces applies to these atypical models as well. The reflection action can change the ordering of standard and thick particles, and thus it encodes the manner in which polytopes of different types glue to tile the space.

**Example 6.14.** The illustration in Figure 14 of five chambers of  $\mathcal{C}(D_{4,1})_{\#}$  shows how the configuration of three (standard) particles and 1 thick particle encodes gluing of faces among different types of chambers either across hyperplanes or antipodal maps. This is done by

the twisting action  $\hat{\sigma}$  of Theorem 5.9. We see the gluing of a face of  $\mathcal{P}D_4$  to a face of  $\mathcal{P}X_4^a$  (a - b) and the corresponding labeled configuration spaces. Another face of this  $\mathcal{P}X_4^a$  attaches to a face of  $\mathcal{P}B_4$  (c - d) which glues to the face of another  $\mathcal{P}B_4$  (e - f). This identification is across the hyperplane  $x_i = 0$ , where  $x_i$  is the label for the thick particle. Finally, this  $\mathcal{P}B_4$  glues to another chamber of type  $\mathcal{P}D_4$  (g - h) through an antipodal map.

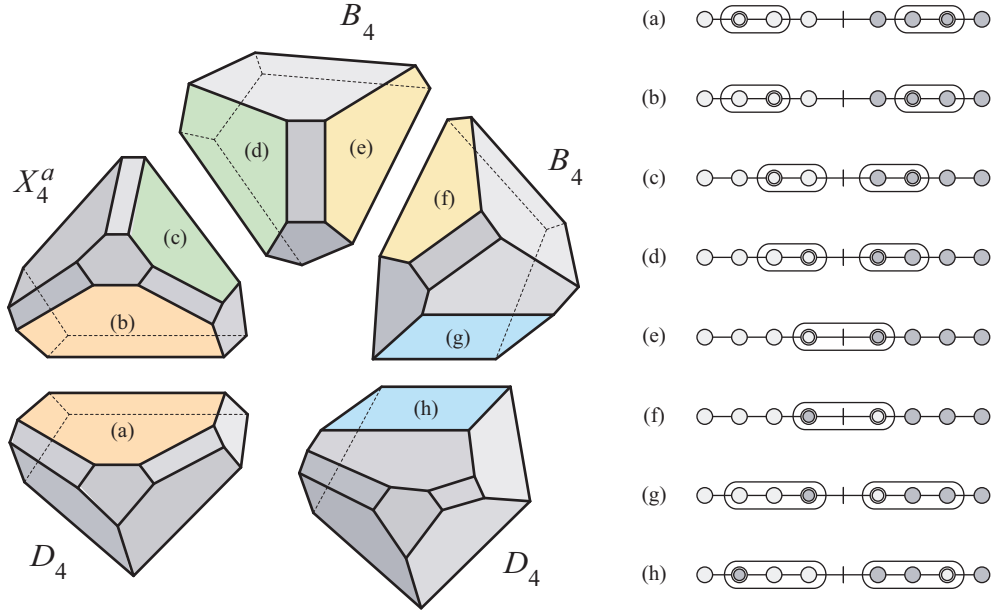


FIGURE 14. Five adjacent chambers in  $\mathcal{C}(D_{4,1})_{\#}$ .

$\mathcal{CW}$	Cellulation	Stabilizer	Enumeration	Configuration
$\mathcal{CA}_n$	$\mathcal{CA}_{k+1}$	$A_{n-k-1}$	$\binom{n+1}{n-k}$	
$\mathcal{CB}_n$	$\mathcal{CB}_{k+1}$	$B_{n-k-1}$	$\binom{n}{n-k-1}$	
	$\mathcal{CB}_{k+1}$	$A_{n-k-1}$	$2^{n-k-1} \binom{n}{n-k}$	
$\mathcal{CD}_n$	$\mathcal{CB}_{k+1}$	$D_{n-k-1}$	$\binom{n}{n-k-1}$	
	$\mathcal{CD}_{k+1,1}$	$A_{n-k-1}$	$2^{n-k-1} \binom{n}{n-k}$	
$\mathcal{CD}_{n,m}$	$\mathcal{CB}_{k+1}$	$D_{n-k-1,r}$	$\binom{m}{r} \binom{n-m}{n-k-r-1}$	
	$\mathcal{CD}_{k+1,m-r+1}$	$A_{n-k-1}$	$2^{n-k-1} \binom{n}{n-k}$	

TABLE 5. Minimal building sets of dimension  $k$  for spherical complexes.

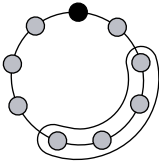
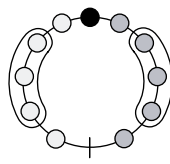
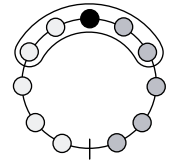
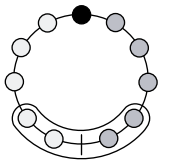
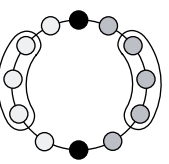
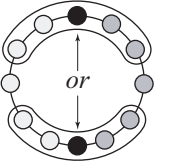
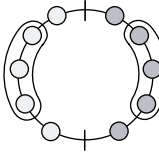
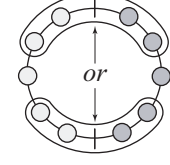
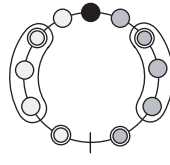
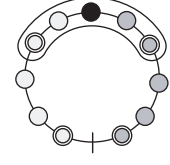
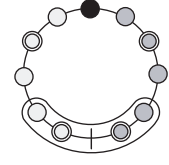
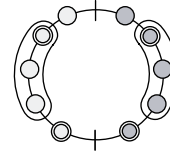
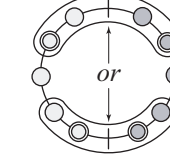
$CW$	$\mathcal{TC}\tilde{A}_n$	$\mathcal{TC}\tilde{B}_n$			$\mathcal{TC}\tilde{C}_n$		
Cellulation	$\mathcal{TC}\tilde{A}_{k+1}$	$\mathcal{TC}\tilde{B}_{k+1,1}$	$\mathcal{TC}\tilde{B}_{k+1}$	$\mathcal{TC}\tilde{C}_{k+1}$	$\mathcal{TC}\tilde{C}_{k+1}$	$\mathcal{TC}\tilde{C}_{k+1}$	
Stabilizer	$A_{n-k}$	$A_{n-k-1}$	$B_{n-k}$	$D_{n-k}$	$A_{n-k-1}$	$B_{n-k}$	
Enumeration	$\binom{n+1}{n-k+1}$	$\binom{n}{n-k}2^{n-k-1}$	$\binom{n}{n-k}$	$\binom{n}{n-k}$	$\binom{n}{n-k}2^{n-k-1}$	$2\binom{n}{n-k}$	
Configuration							
$CW$	$\mathcal{TC}\tilde{D}_n$		$\mathcal{TC}\tilde{B}_{n,m}$			$\mathcal{TC}\tilde{D}_{n,m}$	
Cellulation	$\mathcal{TC}\tilde{D}_{k+1,1}$	$\mathcal{TC}\tilde{B}_{k+1}$	$\mathcal{TC}\tilde{B}_{k,m-r+1}$	$\mathcal{TC}\tilde{B}_{k+1,r}$	$\mathcal{TC}\tilde{C}_{k+1}$	$\mathcal{TC}\tilde{D}_{k+1,m-r+1}$	$\mathcal{TC}\tilde{B}_{k+1,r}$
Stabilizer	$A_{n-k-1}$	$D_{n-k}$	$A_{n-k-1}$	$B_{n-k-1}$	$D_{n-k-1,r}$	$A_{n-k-1}$	$D_{n-k-1,r}$
Enumeration	$2^{n-k-1}\binom{n}{n-k}$	$2\binom{n}{n-k}$	$\binom{n}{n-k}2^{n-k-1}$	$\binom{n-m}{n-k-r-1}\binom{m}{r}$	$\binom{n-m}{n-k-r-1}\binom{m}{r}$	$\binom{n}{n-k}2^{n-k-1}$	$2\binom{n-m}{n-k-r-1}\binom{m}{r}$
Configuration							

TABLE 6. Minimal building sets of dimension  $k$  for Euclidean complexes.

```

Algorithm Tubes(G, k)
01 For i = 1 to n
02   m_i := p_i
03 For each (v_i, v_j) in E
04   m_i := m_i * p_{i,j}
05   m_j := m_j * p_{i,j}
06 M := m_1 * m_2 * ... * m_n
07 For each k-tuple s = (c_1, ..., c_k), with 0 < c_i < M + 1
08   If gcd(c_i, c_j) = 1 OR c_i | c_j OR c_j | c_i for all i,j then
09     For i = 1 to k
10       X_i := {m_j : m_j | c_i}
11       If X_i is nonempty then
12         Pick x_1 in X, Y := {x_1}
13         While X_i \ Y is nonempty
14           Pick y in X_i
15           If there is an x in Y such that gcd(x, y) > 1 then
16             Y := Y + {y}
17           Continue until no more elements of X_i can be added to Y
18         If X_i = Y then
19           Continue to next i
20         Else
21           Continue to next k-tuple
22       Let E_s = {X_1, ..., X_k}
23       If |E_s| = k then
24         Add E_s to the list L if it has not been previously added
25 Output length of L

```

TABLE 7. Algorithm for computing the number of  $k$ -tubings of an arbitrary graph. The  $p_i$  are prime numbers, with  $p_i \neq p_j$  if  $i \neq j$  as strings.

$n$	$A$	$B$	$D$	$\tilde{A}$	$\tilde{B}$	$\tilde{C}$	$\tilde{D}$
2	0	0		-1		2	
3	1	2		0	0	0	
4	0	0	0	9	360	-16	0
5	-3	-16	360	0	0	0	30
6	0	0	0	-225	-40320	720	0
7	45	720	-40320	0	0	0	-2340
8	0	0	0	11025	8346240	-80640	0
9	-1575	-80640	8346240	0	0	0	383040
10	0	0	0	-893025	-2794176000	476872704000	0

TABLE 8. Euler characteristics of compactified Coxeter complexes.

## REFERENCES

1. R. Bott and C. Taubes, On the self-linking of knots, *J. Math. Phys.* **35** (1994), 5247-5287.
2. N. Bourbaki, *Lie Groups and Lie Algebras: Chapters 4-6*, Springer-Verlag, Berlin, 2002.
3. K. S. Brown, *Buildings*, Springer-Verlag, New York, 1989.
4. M. Carr, S. Devadoss, Coxeter complexes and graph-associahedra, preprint 2004.
5. M. Davis, T. Januszkiewicz, R. Scott, Nonpositive curvature of blowups, *Selecta Math.* **4** (1998), 491 - 547.
6. M. Davis, T. Januszkiewicz, R. Scott, Fundamental groups of minimal blow-ups, *Adv. Math.* **177** (2003), 115-179.
7. C. De Concini and C. Procesi, Wonderful models of subspace arrangements, *Selecta Math.* **1** (1995), 459-494.
8. B. DeMedeiros, personal communication 2003.
9. S. Devadoss, A space of cyclohedra, *Disc. Comp. Geom.* **29** (2003), 61-75.
10. S. Devadoss, Combinatorial equivalence of real moduli spaces, *Notices Amer. Math. Soc.* **51** (2004), 620-628.
11. W. Fulton and R. MacPherson, A compactification of configuration spaces, *Ann. Math.* **139** (1994), 183-225.
12. M. M. Kapranov, The permutoassociahedron, MacLane's coherence theorem, and asymptotic zones for the KZ equation, *J. Pure Appl. Alg.* **85** (1993), 119-142.
13. M. Markl, S. Shnider, J. Stasheff, *Operads in Algebra, Topology and Physics*. Amer. Math. Soc., Rhode Island, 2002.
14. J. D. Stasheff, Homotopy associativity of  $H$ -spaces, *Trans. Amer. Math. Soc.* **108** (1963), 275-292.

S. ARMSTRONG: WILLIAMS COLLEGE, WILLIAMSTOWN, MA 01267  
*E-mail address:* `suzanne.m.armstrong@williams.edu`

M. CARR: UNIVERSITY OF MICHIGAN, ANN ARBOR, MI 48109  
*E-mail address:* `mpcarr@umich.edu`

S. DEVADOSS: WILLIAMS COLLEGE, WILLIAMSTOWN, MA 01267  
*E-mail address:* `satyan.devadoss@williams.edu`

E. ENGLER: WILLIAMS COLLEGE, WILLIAMSTOWN, MA 01267  
*E-mail address:* `eric.h.engler@williams.edu`

A. LEININGER: MIT, CAMBRIDGE, MA 02139  
*E-mail address:* `anandal@mit.edu`

M. MANAPAT: UC, BERKELEY, CA 94720  
*E-mail address:* `manapat@ocf.berkeley.edu`